university of groningen

University Medical Center Groningen

University of Groningen

Optical absorption in TiNxOy-compounds

Vogelzang, E.; Sjollema, J.; Boer, H. J.; de Hosson, J. Th. M.

Published in:
Journal of Applied Physics

DOI:
10.1063/1.338370

IMPORTANT NOTE: You are advised to consult the publisher's version (publisher's PDF) if you wish to cite from it. Please check the document version below.

Document Version
Publisher's PDF, also known as Version of record

Publication date:
1987

Link to publication in University of Groningen/UMCG research database

Citation for published version (APA):
Vogelzang, E., Sjollema, J., Boer, H. J., & de Hosson, J. T. M. (1987). Optical absorption in TiNxOy-compounds. *Journal of Applied Physics*, *61*(9), 4606-4611. https://doi.org/10.1063/1.338370

Copyright
Other than for strictly personal use, it is not permitted to download or to forward/distribute the text or part of it without the consent of the author(s) and/or copyright holder(s), unless the work is under an open content license (like Creative Commons).

The publication may also be distributed here under the terms of Article 25fa of the Dutch Copyright Act, indicated by the "Taverne" license. More information can be found on the University of Groningen website: https://www.rug.nl/library/open-access/self-archiving-pure/taverne-amendment.

Take-down policy
If you believe that this document breaches copyright please contact us providing details, and we will remove access to the work immediately and investigate your claim.

Downloaded from the University of Groningen/UMCG research database (Pure): http://www.rug.nl/research/portal. For technical reasons the number of authors shown on this cover page is limited to 10 maximum.

Download date: 04-05-2023

Optical absorption in TiN_xO_y-compounds

E. Vogelzang, J. Sjollema, H. J. Boer, and J. Th. M. De Hosson
Department of Applied Physics, Materials Science Centre, University of Groningen, Nijenborgh 18, 9747 AG Groningen, The Netherlands

(Received 18 March 1986; accepted for publication 10 December 1986)

Thin films of Ti, TiN_x, and TiN_xO_y were prepared by dc reactive magnetron sputtering. The normal spectral reflectance and transmittance of films were measured in the spectral region of 0.4–25 μm. The free electron contribution to the optical properties has been determined from measurements of the Hall coefficient and the dc resistivity. Optical band-band transitions, that are found in TiN_xO_y, are compared to the calculated band structure of TiN and TiO.

I. INTRODUCTION

Titanium nitrides and oxides have received increasing attention, not only due to their high wear resistance, but also because these materials offer considerable promise for applications as high efficiency solar collectors.[1,2] This paper reports on the optical properties of TiN_xO_y coatings and will emphasize the physical basis for optical absorption. In particular, we have concentrated our work on cases involving a high absorption in the solar part of the spectrum, at wavelengths between 0.4 and 2 μm, and low emission in the thermal infrared region (2–25 μm), by choosing a substrate of high infrared reflectivity overcoated by a material with high solar absorbance and high infrared transparency.

Over the past decades it has been known,[3] that addition of electronegative elements to transition metals will depress the plasma frequency, thereby reducing the reflectivity in the solar part of the spectrum to roughly approximate an ideal spectral profile. Until now attempts have been made to improve this spectral profile by choosing various transition-metal combinations with electronegative elements. We have tried to describe the underlying physical principles, that take part in this absorption process, not only by taking into account the free electron terms and relaxation times but also by calculating electron band energies which provide information about transition energies of the material. Moreover, we concentrated on the question of why the conductivity of thin TiN_xO_y single layers substantially decreases with increasing oxygen content.

II. METHODS

A. Experiment

Thin films are deposited on borosilicate glass substrates by dc reactive magnetron sputtering at a base gas pressure of about 2×10^{-4} Pa. Near-stoichiometric TiN films are obtained at an argon pressure of 0.2 Pa and a reactive nitrogen pressure of 0.07 Pa. The acceleration voltage was 450 V, yielding a deposition rate of 1.7 nm/s at a discharge current of 2 A.

In order to measure Hall coefficients, extremely thin layers ($\sim$0.06 μm) are needed. Masks were designed in order to optimize the form factors of the layers and to minimize the influence of contacts on the electric field lines. Hall measurements were carried out by making use of slowly alternating current to minimize the Ettinghausen effect.[4] This also allows the use of phase sensitive detection methods accurate enough to determine Hall coefficients. The offset between two voltage contacts is avoided by employing a third contact; external resistance between two contacts can be manipulated in this configuration so that, in the absence of a magnetic field, the offset voltage is zero.

The magnetic field can be varied between -1 and 1 T, the current through the layer was effectively 20 mA; detected Hall voltages varied between 5×10^{-5} and 5×10^{-6} V. Reflection and transmission measurements on these layers were performed in the spectral region of 0.4–25 μm.

B. Methods of calculation

Recently, Williams *et al.*[5] presented a conceptual model and computational procedure for the study of the electronic structure of metallic compounds. The model adopts hydrostatic pressure as a tool for the analysis of cohesion (see Ref. 6). The basic idea behind the use of hydrostatic pressure to analyze cohesion is that the total energy differences between a free atom and one compressed into a solid can be represented as the integral of the pressure, which must be exerted on the surface of the atomic cell. The advantage of this approach over the direct calculation and subtraction of total energies is that it provides an identification of the role played in the binding process by *s*, *p*, and localized *d* electrons. The model involves no adjustable or experimentally derived parameters. All contributions to the total energy are obtained from independent compressed-atom calculations. The state of the compressed atoms is obtained from energy band calculations, which were carried out by Williams and co-workers using a new method: the augmented-spherical-wave method (ASW). This procedure is related to the linear-muffin-tin orbitals technique[7] and is conceptually similar to the augmented-plane-wave technique (APW) developed by Slater.[8] The objective of these methods is the approximate determination of the eigenfunctions and eigenvalues of the single particle Schrödinger equation. A self-consistent field procedure requires the repeated solution of the Schrödinger equation. The total calculation is divided into intra and interatomic parts. The total energy E, written within the density-functional formalism[9]:

$$E_T = E_k + E_{\rm es} + E_{\rm xs},$$

can be expressed as a sum over the compressed atoms E_i^A, plus a Madelung contribution E^m:

 0021-8979/87/094606-06$02.40 © 1987 American Institute of Physics

Downloaded 09 Oct 2006 to 129.125.25.39. Redistribution subject to AIP license or copyright, see http://jap.aip.org/jap/copyright.jsp

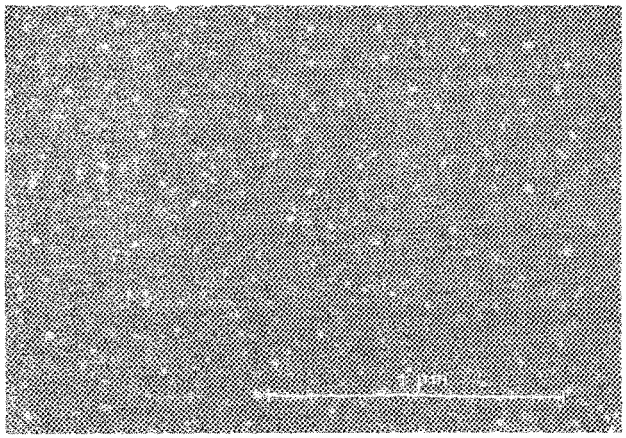

FIG. 1. Dark field picture of TiN_xO_y.

$$E_T = \Sigma_i E_i^A + E^m,$$

where E_k is the kinetic energy of the system of noninteracting electrons, E_{es} represents the electrostatic energy which is the sum of electron-electron and nucleus-nucleus contribution. E_{xs} is the contribution of exchange and correlation effects to the total energy.

III. RESULTS

A. Experiment

1. Lattice structure

First the structure of a TiN_xO_y layer is investigated by means of electron microscopy. From dark field and diffraction pictures it is concluded that the layer has a microcrystalline structure with a grain size of ± 200 Å (far larger than the electron mean free path and so probably not of importance to the resistivity) (see Figs. 1 and 2). The lattice of the grain is evidently that of NaCl: Two interpenetrating fcc sublattices are comprised only of titanium and of either nitrogen or oxygen.

Pictures of layers with only oxygen as a reactant show a rather amorphous structure; however, the lattice turned out to be that of anatase TiO_2 based on an x-ray diffraction measurement (Fig. 3). The grains are far smaller than those of TiN_xO_y and may influence the resistivity. Layers with increasing oxygen content could precipitate into areas of TiO_2, thereby explaining the drastically increased resistivity. This precipitation process in areas with high electrical resistivity is, however, not confirmed by our diffraction measurements.

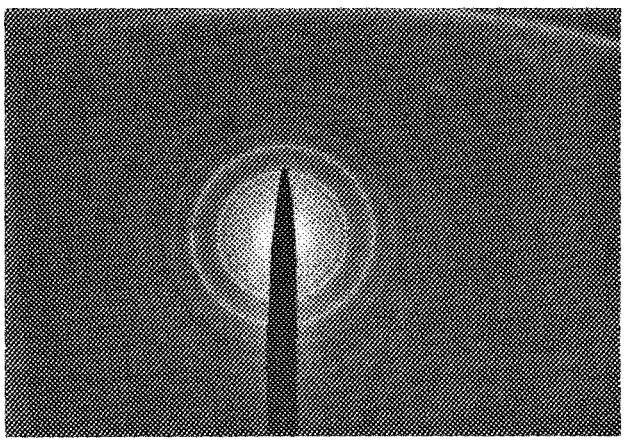

FIG. 2. Diffraction pattern of TiN_xO_y, showing an NaCl lattice (two interpenetrating fcc sublattices).

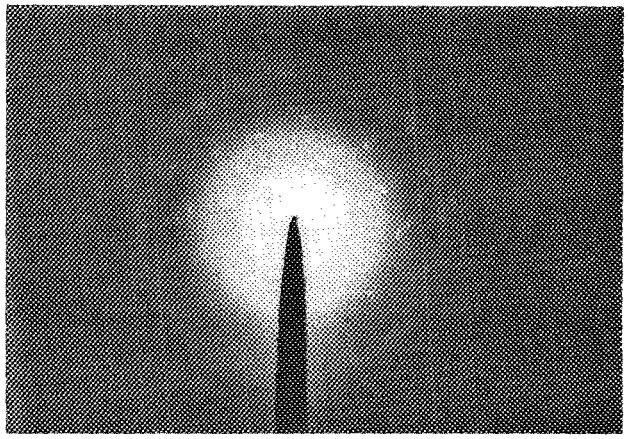

FIG. 3. Diffraction pattern of TiO_2 anatase shows rather amorphous rings together with crystalline or bicrystalline salt spots (the layer was deposited on monocrystalline salt, fractions of which were still present on the specimen).

2. Hall and conductivity measurements

Hall coefficients were measured for three different types of sputtered layers: Ti, TiN, and TiN_xO_y. These layers were characterized by their color, increasing resistivity, and decreasing capacity. Their thickness was measured using interference microscopy. In the case of pure Ti, a small Hall coefficient of -2.0×10^{-11} C/m^3 was found. From x-ray diffraction experiments an hcp lattice with $a_0 = 0.296$ nm and $C_0 = 0.472$ nm has been found for sputtered titanium layers. From the lattice constants of Ti and from the free electron density obtained from our Hall measurements, we obtain 5.4 conduction electrons per Ti atom. This high number can be explained by assuming conduction is partly caused by holes. This was confirmed by earlier measurements of the Hall coefficient of Ti,[10,11] resulting in small positive values. The differences in sign as compared to our measurements are probably due to differences in impurity concentrations in the samples.

In the case of TiN and TiN_xO_y, the magnitudes of the Hall coefficients have been found larger than for pure Ti and we assume only electron conduction is taking place. The oxygen causes a decrease of the conduction electron density (Table I). This is not surprising, since values for TiO show that hole conduction is predominant in this material.[12,13]

With the determination of resistivity of the particular layer we were able to estimate the plasma frequency ω_p and the relaxation time τ which enter in a harmonic oscillator model for $\tilde{\epsilon}$.

$$\tilde{\epsilon}(\omega) = 1 + \sum_{j=1}^{N} \frac{\omega_{pj}^2}{\omega_{0j}^2 - \omega^2 + i\omega/\tau_j}. \quad (1)$$

Downloaded 09 Oct 2006 to 129.125.25.39. Redistribution subject to AIP license or copyright, see http://jap.aip.org/jap/copyright.jsp

TABLE I. Properties of Ti, TiN, and TiN_xO_y films. d = thickness, ρ = resistivity, R_H = Hall coefficient, λ_c = characteristic wavelength, λ_p = plasma wavelength, and n = number of free electrons per molecule.

	Color	$d(\mu m)$	$\rho(\mu\Omega m)$	$R_H(m^3/c)$	$\lambda_c(m)$	$\lambda_p(m)$	n
Ti	silver	0.07	1.2	-2.0×10^{-11}	...	...	...
TiN	gold	0.05	0.8	-9.1×10^{-11}	1.3×10^{-8}	1.4×10^{-7}	1.0
TiN_xO_y	green/opaque	0.07	35	-2.8×10^{-10}	5.9×10^{-7}	2.1×10^{-7}	0.4

Using only the first term together with $\omega_{0j}=0$, we obtain the Drude model describing the free electron contribution to $\tilde{\epsilon}(\omega)$:

$$\tilde{\epsilon}(\omega)=1-(\omega_p^2/\omega^2-i\omega/\tau). \tag{2}$$

The terms ω_p and τ were deduced from the electrical measurements (for the calculation of ω_p we used $m^*=m$). Higher terms in Eq. (1) describe the influence on the dielectric constant of N interband transitions: ω_{pj} is the oscillator strength, ω_{0j} the resonance frequency, and τ_j the damping factor of the jth transition. For convenience we will write the harmonic oscillator model in terms of wavelengths:

$$\tilde{\epsilon}(\lambda)=1+\sum_{j=1}^{N}1\Big/\left(\frac{1}{E_j}-\frac{\lambda_{pj}^2}{\lambda^2}+\frac{i\lambda_{cj}}{\lambda}\right)$$

with

$$\frac{1}{E_j}=\frac{\omega_{oj}^2}{\omega_{pj}^2}\neq 0 \quad \text{for } j>1,$$

$\lambda_{pj}=2\pi c/\omega_{pj}$: plasma wavelength,

$\lambda_{cj}=2\pi c/(\omega_{pj}^2\tau_j)$: characteristic wavelength.

In Table I the plasma wavelength and characteristic wavelength for TiN and TiN_xO_y together with their resistivity ρ, color, Hall coefficient R_H, number of free electrons per molecule n, and thickness d are listed.

3. Optical measurements

Reflectivity and transmission of TiN and TiN_xO_y were measured in order to investigate the manner in which optical characteristics are controlled by free electrons. Therefore, we fitted one or more plasma and characteristic wavelengths in our harmonic oscillator model to the reflection and transmission measurements. In the case of TiN, it is possible to approximate the measured reflectivity by a single Drude term, adding $\epsilon(\infty)$ as a single fitting parameter by choosing $1/E_2=0.15$ in Eq. (3). This will only affect the reflectivity in the high-frequency range ($<0.8\,\mu m$). The optical properties of TiN in the wavelength region of interest are, therefore, determined by free electrons: only high-energy transitions take place (Fig. 4).

It is possible, however, that lower-energy transitions and their optical effects are dominated by high reflectivity in the solar and infrared region due to free electrons. Transmission and reflection measurements for TiN_xO_y show different features (Fig. 5). Free electron terms do not fully de-

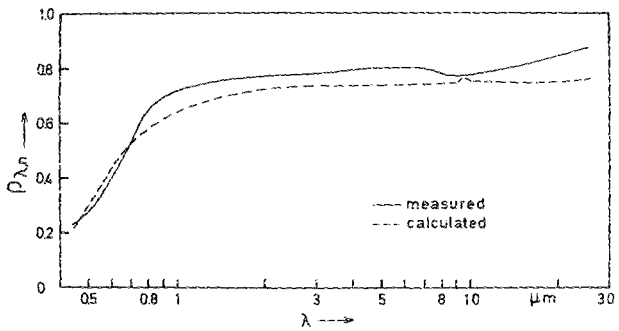

FIG. 4. Reflection characteristic of TiN together with a calculated free electron curve. [The parameter $1/E_2$ was set at 0.15 in Eq. (3) for the calculated fit.]

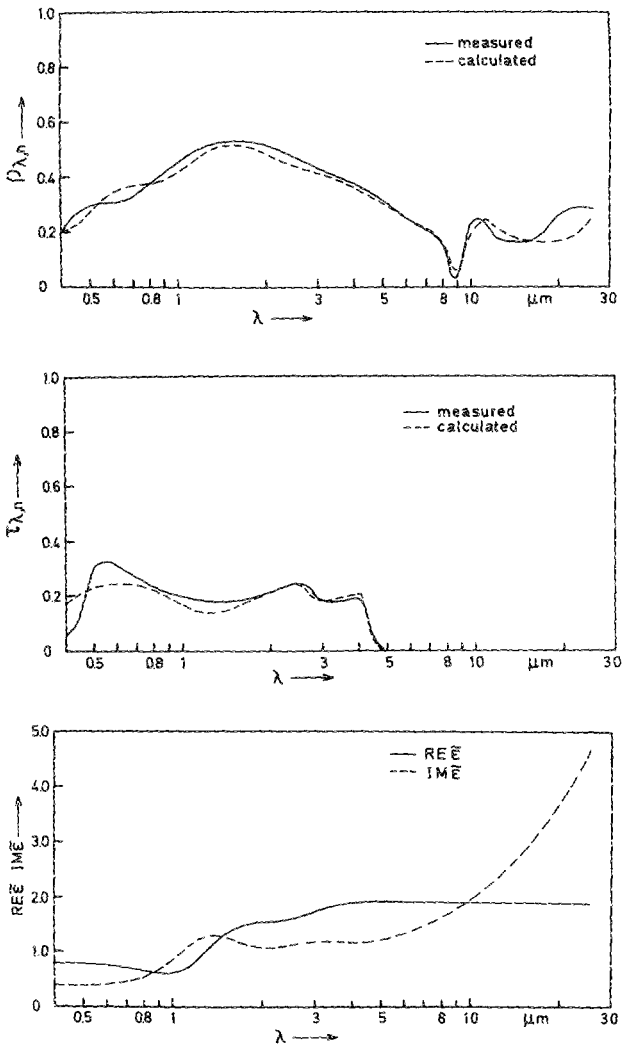

FIG. 5. Reflection (a) and transmission (b) of TiN_xO_y together with a fitted curve. A plot of $\tilde{\epsilon}$ fitted to the reflection and absorption characteristics of TiN_xO_y. Evidently a resonance appears at 1,2 μ.

Downloaded 09 Oct 2006 to 129.125.25.39. Redistribution subject to AIP license or copyright, see http://jap.aip.org/jap/copyright.jsp

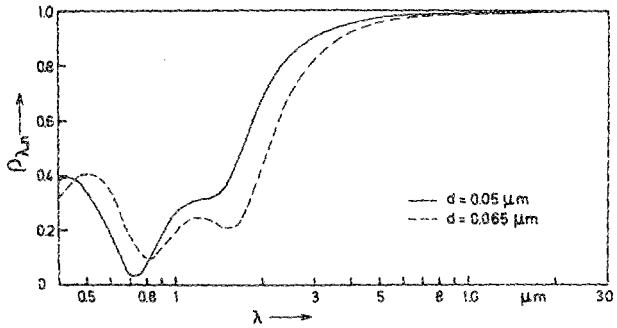

FIG. 6. Reflection curve of a TiN_xO_y layer on a reflective Cu surface. Reflection at 1,2 μ shows a ridge of considerable reflective power. Layers of two different thicknesses are shown.

scribe the optical response of the layer; higher order terms corresponding to optical band-band transitions have to be included as well. A plot of $\tilde{\epsilon}$, which fits the optical measurements, clearly shows a resonance at 1.2 μm, which corresponds to a transition at 1.1 eV. Calculating only with Drude terms, we get a totally opaque layer. Structure in the reflection and transmission spectra results from transitions in the visible and ultraviolet regions. Due to the complexity of the electronic structure of the material, the optical spectrum lacks the features of Lorentzian line shapes. A ridge, however, at $\sim 1.2\,\mu$m in the reflection spectrum characteristic of a TiN_xO_y layer on a high reflective Cu substrate, is apparently due to a resonance in $\tilde{\epsilon}$. This ridge is one of the most

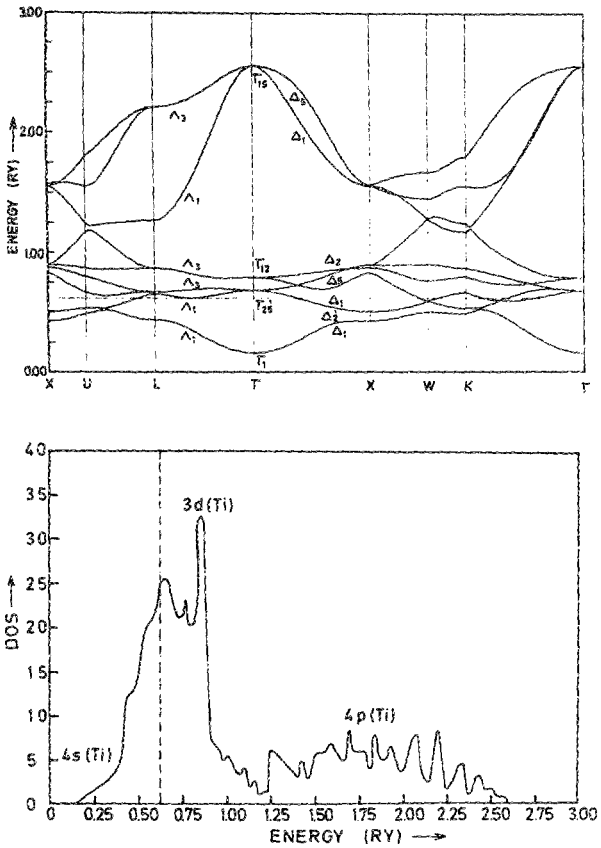

FIG. 7. Bandstructure (a) and density of states (b) of Ti.

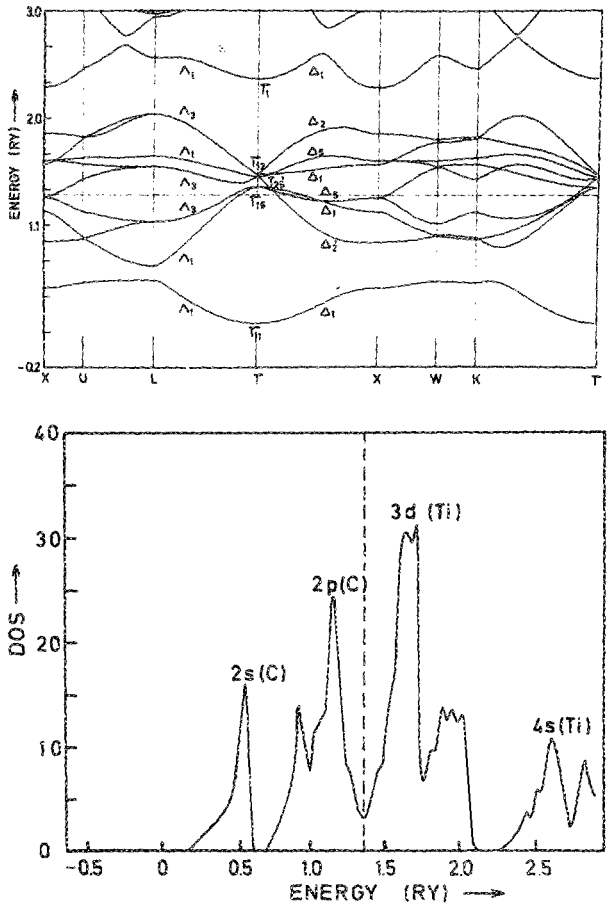

FIG. 8. Bandstructure (a) and density of states (b) of TiC.

complex problems to understand in the realization of high spectral selectivity (Fig. 6).

B. Bandstructure calculation

1. Cohesive and electronic properties

The calculated electronic bandstructures and densities of state of four different materials Ti, TiC, TiN, and TiO are depicted in Figs. 7–10. (In the case of Ti, an fcc lattice was taken instead of an hcp lattice.) Band shifts were investigated while going towards higher electronegativity of the reactants C, N, and O.

In Figs. 7–10, the shifts of the 3*d* bands downwards through E_F are clearly shown by continuously adding electrons to the system. 4*s* electrons in Ti are transferred to 2*p* bands of the electronegative reactants; the band energy is lowered due to increasing attraction in the series C→N→O. 3*d* orbitals are hybridized to a varying degree with 2*p* wave functions of C, N, or O, forming a bonding orbital filled by 2*p* and 3*d* electrons (Figs. 11 and 12 show this hybridization in a plot of the partial states). From these figures it may be concluded that, besides a transfer of 4*s* electrons on Ti to O-2*p* levels, Ti-3*d* electrons are transferred since they are not as tightly bound. Our band calculations on TiN, TiC, and TiO show strong similarities to the calculations of Ern and Switendick[14] on these materials using APW. Only small differences can be noticed in the position of the hybridized 3*d* bands relative to the Fermi surface.

Downloaded 09 Oct 2006 to 129.125.25.39. Redistribution subject to AIP license or copyright, see http://jap.aip.org/jap/copyright.jsp

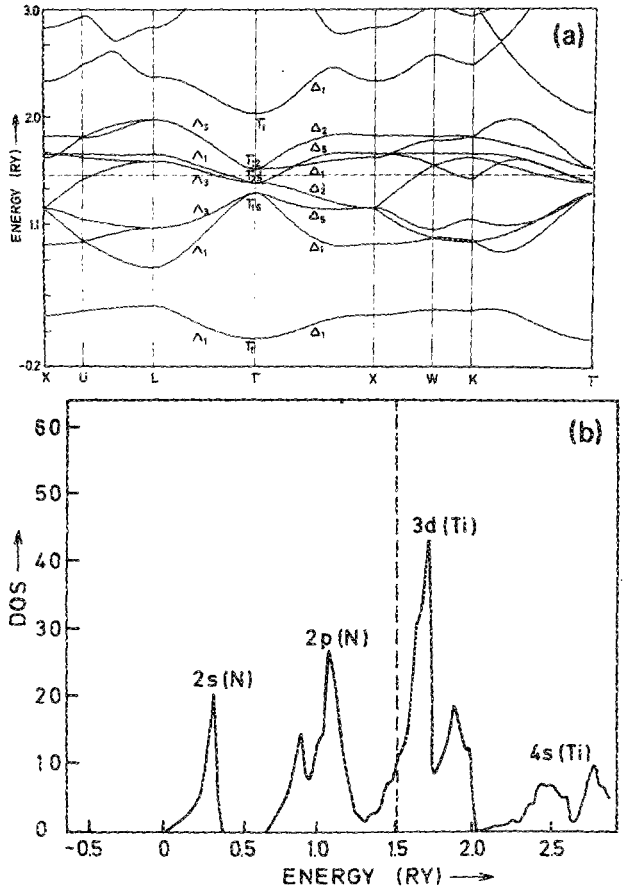

FIG. 9. Bandstructure (a) and density of states (b) of TiN.

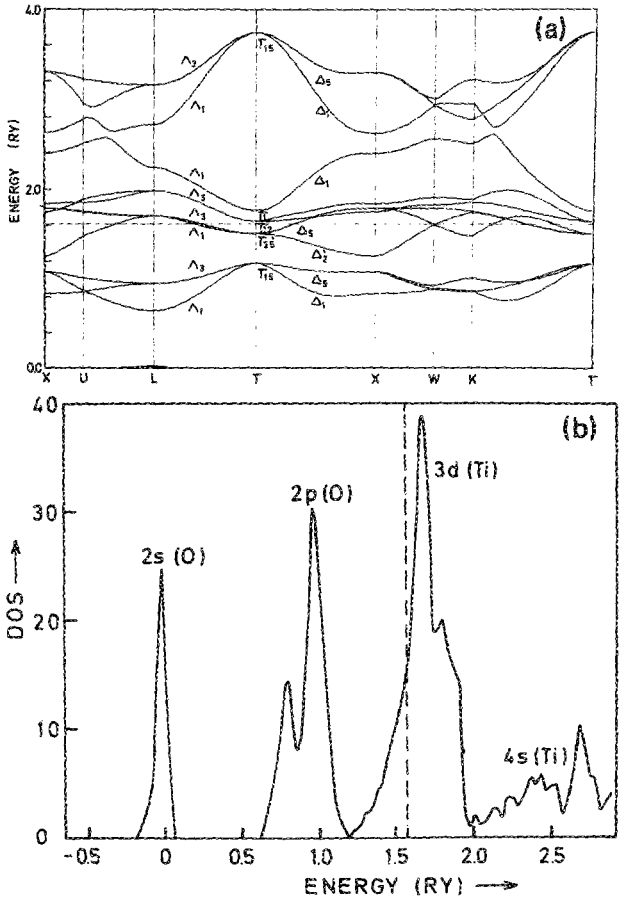

FIG. 10. Bandstructure (a) and density of states (b) of TiO.

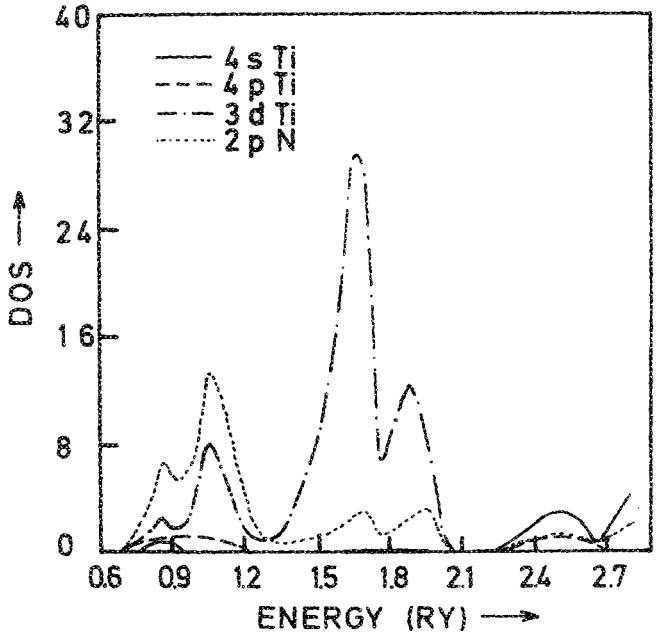

FIG. 11. Partial density of states of TiN showing the hybridized 3*d* orbitals.

Our calculations also lead to self-consistency in ion charge, which enables us to be more explicit about cohesive properties of the materials. Calculated shifts of 4*s* and 2*p* orbitals together with the formation of bonding orbitals lead to covalent bonding. Beside this atomic charge transfer, we can distinguish a spatial charge transfer leading to a Madelung energy and ionic bonding.

Calculations by Conklin and Silversmith[15] on Ti also iterated to self-consistency in ion charge and lead to the same binding mechanisms. (Noteworthy in Table II is a considerable decrease of ion charge at increasing electronegativity of the reactants.) Estimate of the electron concentration by

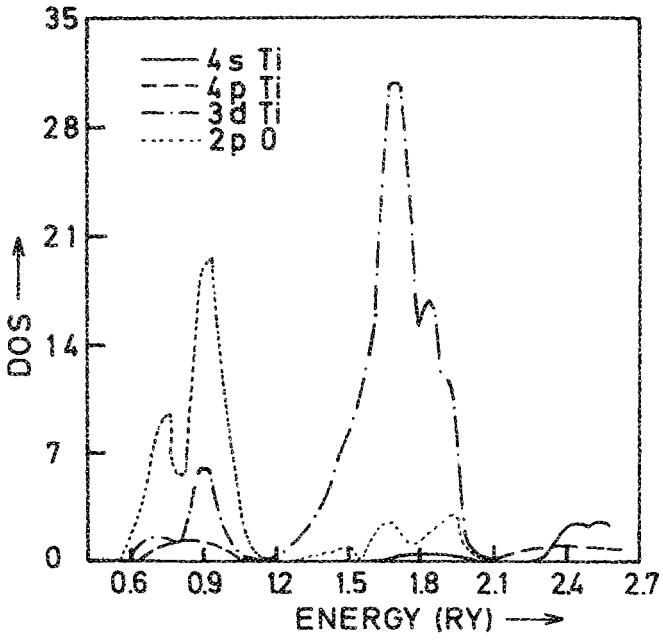

FIG. 12. Partial density of states of TiO showing hybridized 3*d* orbitals.

Downloaded 09 Oct 2006 to 129.125.25.39. Redistribution subject to AIP license or copyright, see http://jap.aip.org/jap/copyright.jsp

TABLE II. Calculated total variational energies, self-consistent ion charge and Madelung energies for Ti, TiC, TiN, and TiO.

	Total var. energy (Ryd)	Self-consist. ion charge (C)	Madelung energy (Ryd)
Ti	− 1695.03	0	0
TiC	− 1771.71	0.49	− 0.18
TiN	− 1804.97	0.44	− 0.17
TiO	− 1845.63	0.32	− 0.09

calculating the volume enclosed by the Fermi surface is omitted, as well as the determination of $m^* = \hbar^2(d^2E/dk^2)^{-1}$. Partial hole conduction in Ti might be explained by strong negative curvature of $3d$ energy bands (hole pockets) near the Fermi surface.

Mott's suggestion that resistivity involves scattering of s electrons on partly filled d bands might also be applied to scattering of d electrons on d sites. The density of possible d sites in TiO is two times higher than TiN which together with the decrease of free electrons in TiO partly explains the poor conducting properties of TiO and to a lesser extent TiN_xO_y.

2. Transitions

The strongly lowered $4s$ band in TiO will lead to a weakly allowed $3d$-$4s$ transition at Γ (eventually via hybridized $2p$ state in the bonding orbital) at 3.8 eV (0.4 μm). Unfortunately, we were not able to experimentally detect an optical transition at this frequency and wavelength just at the edge of the measurement interval. The resonance in $\tilde{\epsilon}$ fitted to transmission and reflection measurements (Fig. 5) at 1.1 eV might correspond with a weakly allowed hybridized $3d$ transition at Γ ($\Gamma'_{25} - \Gamma_{12}$). For TiN we find a transition energy of 1.3 eV. For TiO this transition should take place at 1.9 eV. Transitions in TiN_xO_y possibly take place at a value somewhere between these two energy values. The reason, that we do not notice experimentally any transitions in this energy range in TiN is the predominant role that free electrons play in the optical mechanism.

IV. CONCLUSIONS

Optical properties of TiN between 0.4 and 25 μm can be described by considering free electron terms in a harmonic oscillator model for $\tilde{\epsilon}$. With increasing oxygen content we have to include transition terms too; free electron terms are even increasingly less important.

Obvious is a transition at 1.1 eV which takes place in TiN and in TiN_xO_y; in the case of TiN, however, the free electron reflection dominates transition effects. Band structure calculations only give a qualitative insight in the electrical properties of Ti, TiN, and TiO. The increasing resistivity in this series can be explained from a higher density of states at the Fermi surface for TiO.

Cautious quantitative conclusions can be made about possible transitions: $3d \rightarrow 4s$ ($\Gamma'_{25} \rightarrow \Gamma_1$) partly via $2p$ at 3.8 eV and $3d$ ($2p$) $\rightarrow 3d$ ($2p$) ($\Gamma'_{25} \rightarrow \Gamma_{12}$) at 1.3 eV. It might be concluded that optical transitions in TiO are taking place more strongly than in TiN because of the substantially lowered $4s$ band.

The measured resonance at 1.1 eV is possibly caused by the hybridized $3d$ ($2p$) transitions. The ridge in the reflection characteristics of TiN_xO_y layers on Cu is due to the same transition.

ACKNOWLEDGMENT

The work is supported by the Foundation for Fundamental Research on Matter.

[1] J. Lafait, J. M. Behagel, S. Berthier, and J. Rivory, J. Phys. (Paris), Colloq. **C1**, 133 (1981).
[2] L. Roux, J. Hanus, J. C. Francois, and M. Sigrist, Sol. Energy Mater. **7**, 299 (1982).
[3] R. E. Hahn and B. O. Seraphin, in *Physics of Thin Films*, Vol. 10, edited by G. Hass (Academic, New York, 1978).
[4] O. Lindberg, Proc. IRE, 1414 (1952).
[5] A. R. Williams, J. Kübler, and C. D. Gelatt, Phys. Rev. B **19**, 6094 (1979).
[6] D. G. Pettifor, Commun. Phys. **1**, 141 (1976).
[7] O. K. Andersen, Phys. Rev. B **12**, 3060 (1975).
[8] J. C. Slater, Phys. Rev. **92**, 603 (1953).
[9] P. Hohenberg and W. Kohn, Phys. Rev. B **136**, 864 (1964).
[10] G. W. Scovil, J. Appl. Phys. **24**, 226 (1953).
[11] S. Foner, Phys. Rev. **91**, 447 (1953).
[12] A. A. Somokhalev and A. G. Rustamov, Sov. Phys.-Solid State **5**, 877 (1963).
[13] L. V. Dmitrieva, V. A. Ioffe, and I. B. Patrina, Sov. Phys.-Solid State **7**, 2228 (1966).
[14] V. Ern and A. C. Switendick, Phys. Rev. **137**, 202 (1965).
[15] J. B. Conklin and D. J. Silversmith, Int. J. Quantum Chem. **5**, 243 (1968).

Downloaded 09 Oct 2006 to 129.125.25.39. Redistribution subject to AIP license or copyright, see http://jap.aip.org/jap/copyright.jsp